Defect complexes and cluster doping of InN: First-principles investigations

X. M. Duan and C. Stampfl
School of Physics, The University of Sydney, Sydney, New South Wales 2006, Australia
(Received 1 May 2008; published 27 January 2009)

We perform first-principles density-functional theory calculations to investigate the atomic and electronic properties and the formation energies of different defects and dopant complexes (involving V_N, V_{In}, O, Si, Mg, and C) in wurtzite InN. We find that O substituted on a N site (O_N) and Si substituted on an In site (Si_{In}) are the most favorable sites for O and Si impurities, which act as single donors, with the ionized state (O_N^+ and Si_{In}^+) being most stable in *p*-type InN. Substitutional C on a N site (C_N) and Mg on an In site (Mg_{In}) are the most favorable sites for the C and Mg impurities, which are predicted to be single acceptors under more *n*-type conditions. Two O, Si, and Mg atoms in the neutral and charged states prefer to be well separated, exhibiting a mutually repulsive interaction, as do two C atoms in the charged state. Two carbon atoms in the neutral state, however, prefer to be located on neighboring anion sites. We also investigate defect complexes involving vacancies and impurities, as well as defect configurations arising from "codoping" and/or "cluster-doping" concepts, namely, Mg_mO_n $(m,n \leq 4)$ and Si_iC_j $(i,j \leq 4)$ complexes. Rather than being isolated defects, the nitrogen vacancy V_N prefers to be bound to Mg_{In}, forming a neutral $Mg_{In}V_N$ complex, while the indium vacancy V_{In} prefers to bond to oxygen, but the formation energy for the O_NV_{In} complex (in all charge states) is high. The formation energy of the $3O_NV_{In}$ complex is significantly lower, but is still too high to be an important defect in InN in equilibrium. Our results indicate that the Mg_mO_n complexes could be important defects under both In-rich and N-rich conditions: for *p*-type material, donor defects containing more O than Mg have very low formation energies, while for *n*-type material, acceptor defects containing more Mg than O have low formation energies. These complexes could provide a more efficient *p*- (or *n*-) type doping than single Mg (or than single Si and O). Our results suggest complexes of Si_iC_j, on the other hand, offer no advantage over single dopants.

DOI: 10.1103/PhysRevB.79.035207 PACS number(s): 71.55.Eq, 71.15.Mb, 61.72.J−

I. INTRODUCTION

Indium nitride is of considerable interest as it possesses a series of outstanding properties,[1–3] such as a small effective mass[4] (leading to a large electron mobility and a high carrier saturation velocity). Therefore, it is expected to be one of the most promising materials for high-speed and high-frequency electronic devices.[5] Recently, the experimental energy-band gap was found to be only ~0.7 eV rather than the previously accepted 1.9 eV (e.g., Ref. 3, and references therein). Reported first-principles theoretical values of the band-gap range from 0–1.55 eV depending on the level of treatment (e.g., Refs. 6–9). The narrow-band gap has generated interest in InN also for applications such as high-efficiency solar cells, light-emitting diodes, and laser diodes. The ability to fabricate both *p*-type and *n*-type InN is essential to the realization of these devices. Despite recent intense investigations, InN remains the least understood material of the group-III-nitride compounds, largely because of the difficulties associated with producing high-quality InN. This is the case despite its use in InGaN ternary systems in optoelectronic components whereby increasing In contents makes it possible to span virtually the entire solar range. Mg has been used to obtain *p*-type GaN and AlN and is thought to also be a *p*-type dopant for InN.[6,10] Early studies of Mg doping of InN did not show *p*-type conduction.[11,12] Very recently buried *p*-type conductivity was reported in Mg-doped InN on the basis of capacitance-voltage photoluminescence and variable magnetic-field Hall-effect measurements.[13,14] A major challenge for the growth of InN is to control the *n*-type conductivity as observed in nominally undoped material. The unintentional introduction of impurities can affect the physical and electronic properties of InN and thus may degrade the performance of devices. Point defects and impurities, such as nitrogen vacancies and oxygen and silicon impurities, are often considered to be responsible for the unintentional *n*-type conductivity.[6,10,15] Oxygen is one of the most common impurities which is frequently present during growth and is the most probable donor which can be easily incorporated into InN as grown by the most popular methods of molecular-beam epitaxy (MBE) and metalorganic vapor-phase epitaxy (MOVPE).[11,16] Silicon doping of $In_xGa_{1-x}N$ multiquantum wells have been used to improve structural and optoelectronic characteristics of the active layer.[17] Silicon is commonly used to achieve *n*-type conductivity in GaN and $Al_xGa_{1-x}N$.[18]

With regard to first-principles investigations, Stampfl *et al.*[6] investigated the atomic and electronic properties of native defects and selected impurities and dopants (O, Si, and Mg) in zinc-blende (zb) InN using density-functional theory (DFT) and the pseudopotential plane-wave method. Similarly to AlN (Ref. 19) and GaN,[20] the N and cation vacancies were found to be the lowest energy native point defects in *p*-type and *n*-type material, respectively, and oxygen and silicon atoms act as donors and can easily be incorporated during growth. The acceptor Mg was found to have a lower formation energy than in GaN, indicating a higher solubility for Mg in InN and InGaN.[6] Residual carbon is often present in InN films during growth via metalorganic chemical vapor deposition, remote plasma-enhanced chemical vapor deposi-

tion, and MBE.[21] However, no theoretical study has been reported for carbon impurities in InN.

Understanding the role of native defects, impurities, and dopants and the interaction between them, in altering the material properties, and eventually controlling of the concentration, are of crucial importance for the growth and fabrication of group-III-nitride containing electronic and optoelectronic devices. The impurities (O, Si, Mg, and C) and their related complexes in GaN and AlN have been investigated based on DFT calculations: Stampfl and Van de Walle[19] found that the dopants or impurities O and Si are shallow donors with very low formation energies in *p*-type material and that Mg is a shallow acceptor. It was suggested that the nitrogen vacancy in wurtzite (wz)-AlN (and in addition the Al interstitial in zb-AlN) may act to compensate the Mg acceptor in *p*-type AlN. For the defect complexes $Mg_{Al}O_N$ (MgO) and $2(Mg_{Al}O_N)$ (Mg_2O_2) in zb-AlN, they found that the binding energy (1.6 eV) and formation energy (1.67 eV) of Mg_2O_2 are larger than those of MgO (0.6 and 0.92 eV, respectively); thus MgO pairs may be more abundant due to the lower formation energy. A binding energy of 0.6 eV for the MgO complex in zb-GaN was also reported.[22] More recently, Mg_nO ($n=2,3,4$) complexes in wz-AlN were investigated on the basis of *ab initio* calculations, and it was proposed that due to the associated lower activation energies compared to isolated Mg acceptors, higher hole concentrations may be achieved by Mg:O.[23] Gorczyca *et al.*[24] investigated $Mg_{Ga}O_N$ and $Mg_{Ga}V_N$ structures in zb-GaN and proposed that such complexes could play a role in self-compensation when attempting *p*-type doping, which could also have implications for InN. In earlier work, Neugebauer and Van de Walle[20] studied Ga vacancy related complexes, which are responsible for the infamous yellow luminescence in GaN, and found that $V_{Ga}O_N$ is much more stable than $V_{Ga}Si_{Ga}$. Mattila and Nieminen[25] showed that the cation-vacancy-related complexes ($V_{Ga}O_N$ and $V_{Al}O_N$) are energetically very favorable defects in zb-GaN and zb-AlN and induce gap states that are very likely to take part in the yellow luminescence or violet luminescence emission. Wright[26] investigated defect complexes involving O (MgO, SiO, and $V_{Ga}O_N$) in wz-GaN and found that $(Mg_{Ga}O_N)^0$, $(Si_{Ga}O_N)^-$, and $(V_{Ga}O_N)^{2-}$ can exist in equilibrium. Carbon has been found to be a shallow acceptor when substituted for nitrogen and a shallow donor when substituted for Al or Ga in wz-AlN and wz-GaN.[27,28] To the best of our knowledge, there is, however, so far no detailed study of the incorporation of these impurities and, particularly the complexes that may form, in wz-InN.

In this paper, we investigate the structural and electronic properties, and formation energies, of impurity and dopant complexes in wz-InN through first-principles DFT calculations. We find that the formation energies of O and Si in the single positive charge state are very low in *p*-type material. Si_{In} is slightly preferred over O_N, representing easily incorporated donors, similar to as found for zb-InN.[7] Carbon and Mg are predicted to be single acceptors, where Mg_{In} is found to lie about 3 eV lower in energy than C_N under N-rich conditions. The ionization energy for the Mg acceptor is lower by 0.16 eV compared to the C acceptor, thus Mg is a more favorable acceptor than C for *p*-type doping under both In- and N-rich conditions. Investigating the interaction between impurities, we find that two O, Si, and Mg atoms prefer to be well separated, exhibiting a mutually repulsive interaction in both the neutral and charged states; in contrast, two nearest-neighboring C atoms are more favorable than the well-separated configurations in the neutral state (though still high in energy), while in the ionized charge state, they prefer to be far apart. We also investigate various impurity complexes involving the nitrogen and indium vacancies, as well as "codoping" and "cluster doping" of Mg_nO_m, and Si_iC_j (with n and $m=1-4$; i and $j=1-4$). [Note, here we use the subscripts m, n, i, and j to indicate the number of Mg, O, Si, and C atoms, respectively, and not the site.] Our results indicate that the nitrogen vacancy binds to magnesium, forming a $Mg_{In}V_N$ complex with a formation energy of 1.57 eV under In-rich conditions. The indium vacancy binds to oxygen, where the O_NV_{In} complex has a high formation energy. The formation energy for the latter complex can be significantly decreased by adding another two oxygen atoms to the complex, i.e., $3O_NV_{In}$, but still the formation energy is high, indicating it is not an important defect in InN in equilibrium. Mg_nO_m codoping or cluster doping could be useful to aid in both *p*-type and *n*-type conduction in InN, while our results indicate that Si_iC_j complexes formation brings no improvement.

II. CALCULATION METHOD

We perform DFT calculations with the ESPRESSO code,[29] using the local-density approximation (LDA) for the exchange-correlation functional and the plane-wave pseudopotential method, with a supercell geometry. We treat the indium 4*d* electrons with the nonlinear core correction (nlcc) (Refs. 30 and 31) and use an energy cutoff of 60 Ry. The optimized wz lattice constants are $a=3.511$ Å, $c/a=1.624$, and $u=0.376$, which compare well with the experimental values (3.533 Å, 1.611, and 0.375).[32] The calculated heat of formation $\Delta H_f=-1.16$ eV is in reasonably good agreement with experimental values which range from −0.22 to −1.49 eV.[32] It is, however, greater than that obtained when including the In-4*d* electrons as valence, where the value is reported to be −0.19 eV for cubic InN.[33] The cohesive energy is calculated to be −10.237 eV where we include the spin-polarization energies of the N and In atoms of 2.925 and 0.076 eV, respectively. The experimental value is −7.97 eV and the obtained value by including In-4*d* electrons as valence is −9.11 eV.[33] Thus the LDA plus nlcc approach overestimate somewhat the cohesive energy and heat of formation as has been discussed in Ref. 33. The band gap is calculated to be 0.65 eV for the nlcc approach and 0 eV when including In-4*d* electrons as valence (except for the value of the band gap, the nlcc and In-4*d* treatments predict very similar band structures for wz-InN bulk). Recent experiments report a band gap of around 0.7 eV,[3,34] but also a value of ~1.4 eV has been reported.[35] Other post-DFT approaches yield band gap values in the range from 0.02 eV to 1.55 eV (Ref. 36) depending upon the particular description.

To investigate the spatial distribution of the impurities, a wz supercell with 96 atoms ($2\sqrt{3}a\times 3a\times 2c$) is used. A re-

ciprocal space **k**-point mesh of $3\times3\times3$ is employed in the calculations. Test calculations which include In-4*d* electrons as valence show consistent results to those of the pseudopotentials used in this paper as will be explained below. Due to the finite cell used in the present calculations, we estimate that the error in the calculated formation energies is about 0.2 eV. However, we expect that the relative trends of the defect formation energies are more accurate.

The formation energy of a complex in a given charge state q can be expressed as

$$E^f[\text{defect}] = E_{\text{tot}}[\text{defect}] - E_{\text{tot}}[\text{InN,bulk}] - \sum_i n_i\mu_i + q[E_F + E_v + \Delta V(\text{defect})], \quad (1)$$

where $E_{\text{tot}}[\text{defect}]$ is the total energy of the supercell containing the defect, and $E_{\text{tot}}[\text{InN,bulk}]$ is the total energy for the equivalent supercell containing only bulk InN. n_i and μ_i are the number and chemical potential of the atoms added to—or taken from—the bulk reference supercell in order to create the defect, respectively. E_F is the Fermi level referenced to the valence-band maximum (VBM) of the bulk. E_v is the bulk VBM and ΔV is a correction term, which can be obtained by aligning the reference potential in the defect supercell with that in the bulk (see Ref. 37 for details).

The atom chemical potentials μ_i depend on the experimental conditions under which the material is grown. For indium-rich conditions $\mu_{\text{In}}=E_{\text{In}}$ (bulk) and for nitrogen-rich conditions $\mu_{\text{N}}=1/2E_{\text{N}_2}$, where E_{In} (bulk) and E_{N_2} are the energy of an In atom in bulk In and the total energy of the nitrogen molecule, respectively. The chemical potential for nitrogen (indium) under In-rich (N-rich) conditions can be determined from the assumption of thermal equilibrium: $\mu_{\text{In}}+\mu_{\text{N}}=\mu_{\text{InN}}$, where μ_{InN} is the chemical potential of InN, which can be taken as E_{InN} (bulk), the total energy of bulk InN stoichiometric unit. For the case of an impurity or a dopant, the chemical potential of these species will also appear. In the present work we consider defects involving O, Si, Mg, and C atoms. Except for specified cases, the atom chemical potentials of O, Si, and Mg are assumed to be determined by thermal equilibrium with In_2O_3, Si_3N_4, and Mg_3N_2, respectively. The carbon chemical potential μ_{C} is taken as the total-energy per carbon atom in the graphite structure.

From the formation energies we calculate the binding energies for charge-conserving reactions involving ionized impurities. The binding energy of the complex (X_1X_2) in the charge state q is defined with respect to the separated defects X_1 and X_2,

$$E_b[(X_1X_2)^q] = E^f[X_1^{q_1}] + E^f[X_2^{q_2}] - E^f[(X_1X_2)^q], \quad (2)$$

where $q=q_1+q_2$, $E^f[X_1^{q_1}]$, and $E^f[X_2^{q_2}]$ are the formation energies of defect X_1 in charge state q_1 and defect X_2 in charge state q_2, respectively. A positive binding energy corresponds to a stable bound complex. The extension to larger complexes $E_b[(X_1X_2\cdots X_n)^q]$ is straightforward.

TABLE I. Calculated lattice constants a and c (in Å) and heat of formation ΔH_f (in eV per stoichiometric unit) for In_2O_3, β-Si_3N_4, α-Mg_3N_2, MgO, and α-SiC. All-electron (AE) DFT-LDA results and experimental values are included for comparison. "pppw" stands for the pseudopotential plane-wave method.

Crystal		a	c	ΔH_f
In_2O_3	Present pppw	10.097		−12.91
	Present AE[a]	10.118		−10.57
	Expt.	10.118[b]		−9.59[c]
β-Si_3N_4	Present pppw	7.599	2.901	−9.52
	Present AE[a]	7.577	2.893	−10.26
	Expt.	7.608[d]	2.911[d]	−7.70[c]
α-Mg_3N_2	Present pppw	9.890		−4.98
	Present AE[a]	9.942		−5.30
	Expt.	9.953[e]		−4.80[c]
MgO	Present pppw	4.197		−6.02
	Present AE[a]	4.166		−6.21
	Expt.	4.2072[f]		−6.23[g]
α-SiC	Present pppw	3.07	5.037	−0.99
	Present AE[a]	3.064	5.015	−1.13
	Expt.	3.076[g]	5.048	−0.63,[h] −1.158[c]

[a]Reference 38.
[b]Reference 39.
[c]Reference 40.
[d]Reference 41.
[e]Reference 42.
[f]Reference 43.
[g]Reference 44.
[h]Reference 45.

III. RESULTS

A. Physical properties of bulk structures

For bixbyite In_2O_3 and β-Si_3N_4 and antibixbyite Mg_3N_2, we use $4\times4\times4$, $6\times6\times6$, and $4\times4\times4$ **k**-point meshes in the unit cells which contain 80, 14, and 80 atoms, respectively. The respective calculated heats of formation are −12.91, −9.52, and −4.98 eV per stoichiometric unit. Here a negative value represents an exothermic system. These values are obtained at the energy cutoff of 80 Ry, and we fully optimize the lattice constants. The results for the bulk systems are listed in Table I, which also shows the values obtained using all-electron (AE) calculations and experiment for comparison. The cohesive energy of bulk In in a body-centered tetragonal structure is calculated to be −3.52 eV with the lattice constants $a=3.011$ Å and $c=4.756$ Å. Here we used a $6\times6\times6$ **k**-point and an energy cutoff 60 Ry. From all-electron *ab initio* LDA calculations,[46] the cohesive energy is −3.25 eV (with the lattice constants $a=3.20$ Å and $c=4.905$ Å) and the experimental value is −2.52 eV (Ref. 47) [$a=3.24$ Å and $c=4.937$ Å (Ref. 48)]. For bulk Si, we obtained an optimized lattice constant of 5.398 Å [experiment, 5.43 Å (Ref. 49)] and a cohesive energy of −5.19 eV; the experimental value is −4.66 eV.[49] The cohesive energy of hexagonal-close-packed Mg is calculated to be −1.79 eV [experiment, −1.52 eV (Ref. 49)] with the lattice parameters $a=3.132$ Å and $c=5.014$ Å [experiment, $a=3.21$ Å and $c=5.21$ Å (Ref. 49)]. We use an $8\times8\times8$ **k**-point mesh and an energy cutoff of 60 Ry for the bulk Si

TABLE II. Calculated bond length b (in Å) and binding energy E_b (in eV per atom) for the N_2 and O_2 dimers. "pppw" denotes pseudopotential plane-wave calculations. All-electron (AE) DFT-LDA results and experimental values are included for comparison.

Dimer		b	E_b
N_2	Present pppw	1.103	5.56
	Present AE[a]	1.102	5.69
	AE[b]		5.80
	Expt.[c]	1.098	4.96
O_2	Present pppw	1.216	3.66
	Present AE[a]	1.212	3.72
	AE[b]		3.80
	Expt.[d]	1.208	2.56

[a]Reference 46.
[b]Reference 50.
[c]Reference 51.
[d]Reference 52.

and Mg calculations. For bulk MgO in the rocksalt structure and α-SiC, the optimized lattice constants and cohesive energies compare well with those obtained using all-electron calculations and experiment (see Table I). Results for the N_2 and O_2 molecules are given in Table II. In calculating the binding energies for the nitrogen and oxygen molecules, spin-polarization energies have been taken into account: for the nitrogen atom it is 2.925 eV and for the oxygen atom it is 1.44 eV.

B. Single dopants/impurities

We first consider the single oxygen, silicon, magnesium, and carbon impurities/dopants in wz-InN. For each impurity atom, we consider two interstitials sites: tetrahedral (T) and octahedral (O) sites. The T site has two nearest neighbors (one cation and one anion) and six next-nearest neighbors (three cations and three anions), while the O site has six nearest neighbors (three cations and three anions). We also consider substitution on the cation and anion sites.

For the O impurity, the most favorable site is substitution on a N site O_N, where the formation energy under In-rich conditions in the neutral charge state is 0.47 eV (0.86 eV for N rich). The formation energies for oxygen in the interstitial T and O sites are 4.50 eV (3.72 eV, N rich) and 5.16 eV (4.38 eV, N rich) respectively, and for substitution of oxygen on an In site, the formation energy is 10.98 eV (9.05 eV, N rich). The present results for oxygen in InN are similar to the results for oxygen in GaN, in that, in the neutral charge state, substitutional oxygen on a N site has the lowest formation energy and substitutional on a metal-atom site has a very high formation energy.[26] We therefore focus on substitutional oxygen on a N site for further calculations. In the O_N substitutional geometry (in the neutral charge state), the "apical" In atom moves outward by 1.67% and the three equivalent "planar" In atoms relax outward by 1.80%. The O impurity O_N induces a singly occupied level, which is a resonance in the conduction band, thus it acts as a donor. In the single positive charge state, there is an outward expansion—away from the oxygen atom—of the position of the nearest single apical In atom of 2.39% and of the three planar In atoms of 2.42%, thus a slightly larger breathing relaxation compared to the neutral state. For cubic GaN and AlN, O_N^+ induces an outward expansion of the nearest four Ga (Al) atoms of 4.2% (3.8%).[19,53]

Silicon has an atomic radius almost twice that of the nitrogen atom, thus it causes a large strain if it replaces a N atom or occupies an interstitial site. Silicon in GaN and AlN has been shown to have the lowest formation energy when occupying the substitutional cation site.[54] For silicon in zb-InN it was assumed to occupy the substitutional In site.[6] We verified that for wz-InN, Si on both interstitial T and O sites is unfavorable in the neutral charge state, with high formation energies (>5.9 eV under In-rich conditions and >7.5 eV under N-rich conditions). Substitutional Si on a N site also has a large formation energy of 5.04 eV under In-rich conditions and 7.75 eV under N-rich conditions. For Si on an In site, the formation energy is just 0.33 and 0.71 eV under In- and N-rich conditions, respectively. Thus, we only further consider silicon substituted on an In site. The Si_{In} defect induces a large inward contraction of the single apical neighboring N atom of 16.40% and of the nearest three planar N atoms by 15.90%. The huge contraction can be understood in that (i) the bond length of Si-N (~1.75 Å) in $\beta-Si_3N_4$ is much shorter than the apical N-In bond distance (2.15 Å) and the planar N-In bond length (2.14 Å) in InN, and (ii) the calculated heat of formation per atom of Si_3N_4 is greater (1.36 eV) than that of InN (0.58 eV), indicating the stronger Si-N bond. While Si_{Al}^+ in zb-AlN induces a relatively small inward relaxation of 5.0% of the neighboring N atoms,[19] the bond length of Si-N is correspondingly only slightly shorter than that of Al-N in bulk. Like oxygen, Si_{In} induces a singly occupied level in the conduction band and thus acts as a donor. In the single positive charge state, Si_{In}^+ induces an inward displacement of the apical O atom of 15.85% and for the three planar O atoms, the inward displacement is 15.36%, thus very similar to the neutral charge state.

Under In-rich conditions, the formation energy of magnesium in the interstitial T site is 3.86 eV and in the O site it is 2.86 eV. Under N-rich conditions, the values are 0.8 eV higher. A Mg atom substituted on a N site has a higher formation energy of 5.19 and 7.13 eV, while Mg occupying the In site has the lowest formation energy of 1.84 and 1.45 eV under In- and N-rich conditions, respectively. Similarly, DFT calculations for GaN show that Si and Mg on cation sites are the lowest energy sites, and the nitrogen substitutional site for Si and Mg, as well as the interstitial configurations, are energetically unfavorable.[55] Mg_{In} acts as a single acceptor, inducing a defect state with a hole below the VBM. The calculated ionization energy for the Mg acceptor is 0.12 eV, in good agreement with the experimentally reported value of ~0.1 eV. In the neutral charge state, the Mg atom induces an inward movement of the neighboring apical N atom of 3.54% and the three planar N atoms of 3.14%. In the single negative charge state, Mg_{In}^- induces an inward displacement of the apical N atom and three planar N atoms of 3.26% and 3.40%, respectively, thus rather similar to the neutral charge

state. The atomic relaxation of Mg in InN is in contrast to Mg in GaN and AlN, where the Mg atom induces a large outward movement of the surrounding N atoms of 10.1% for Mg^0_{Al} and 9.4% for Mg^-_{Al} in zb-AlN (Ref. 19) and an outward movement of the surrounding N atoms of 6.15% for Mg^0_{Ga} in zb-GaN (Ref. 56). The different relaxation modes can be related to the bond length of Mg-N (2.13 Å in Mg_3N_2); in particular, it is shorter than that of N-In in InN by 0.7% but larger than the bond length of Ga-N in GaN by 9.2% and Al-N in AlN by 12.7%.

As found from *ab initio* calculations,[57] carbon substitution on an In site in wz-AlN has been found to induce a defect level ~1 eV below the conduction band. Therefore carbon does not represent a useful donor for AlN. Substitutional and interstitial carbon in wz-GaN has been studied based on DFT, where C_N was found to be a shallow acceptor and predicted to be the dominant configuration for C in GaN.[28] In contrast to C_{Al} in wz-AlN, C_{Ga} was found to be a shallow donor and predicted to be the primary compensating species when growth occurs under N-rich conditions. For the carbon interstitial configuration C_I, the C atom situated near the center of a *c*-axis channel is favored when the Fermi level lies below 0.9 eV; otherwise, the split interstitial configuration with C and a N atom sharing a N-lattice site is favored.[28] However, no theoretical study has hitherto been reported for C impurities in InN. Our calculations show that substitutional carbon on the N site has the lowest formation energy, where the value is 3.17 eV under In-rich conditions and 4.33 eV under N-rich conditions. In the interstitial *T* and *O* sites, the formation energies are 4.49 and 4.54 eV, respectively. In the In site, it is 5.03 eV. Under N-rich conditions, the values for the interstitial sites are the same and the value for substitution on the In site is 1.16 eV lower.

In the N-substitutional site, C_N acts as a single acceptor, inducing a defect state with a hole above the VBM in the neutral charge state. The C acceptor has a higher formation energy than the Mg acceptor, similar to the behavior of these acceptors in GaN.[58] Carbon is similar in size to N and therefore introduces only a small lattice strain when substituting for N. In the neutral charge state, the relaxed C-In bond lengths both in the apical and planar directions are almost the same as the bulk N-In bond lengths. In the single negative charge state, C^-_N induces an inward displacement of the apical In atom and three planar In atoms of 1.2% and 1.4%, respectively, suggesting that the additional electron localized on the C atom attracts the positively charged In atoms. In zb-AlN, for neutral C_N, the Al-C bonds are 3% longer than the corresponding bulk Al-N bond length as calculated by quantum molecular dynamics,[27] and it is found that C_N is a shallow acceptor with an energy level at about 0.4 eV above the top of the valence band. In contrast to C_N, carbon substitution on the In site C_{In} produces substantial lattice strain. In the neutral charge state, the average C-N bonds are 27% shorter than bulk N-In bonds and the adjacent N-In bonds are on average 6% longer. Similar lattice relaxations of C_N and C_{Ga} in GaN have been reported in Ref. 28. C_{In} induces a defect state with one electron occupied at the conduction-band minimum (CBM) and an unoccupied defect state above the CBM (due to the DFT filling), thus it can act as a donor. In the 1+ charge state, the large lattice strain remains. The formation energy of the carbon donor is much higher than those of the Si and O donor and its ionization energy is as deep as 1.3 eV. The results indicate that carbon is not a good donor in InN.

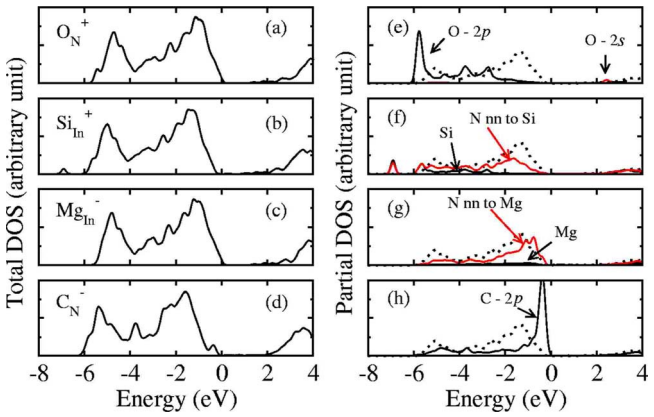

FIG. 1. (Color online) Total DOS (left panel) for (a) O^+_N, (b) Si^+_{In}, (c) Mg^-_{In}, and (d) C^-_N in wz-InN. The corresponding partial densities of states (e)–(h) are shown in the right panel. The zero of energy corresponds to the Fermi level. "nn" represents "nearest neighbor." Dotted lines in the right panel indicate the partial DOS of bulk N atoms.

We have explored the possibility of off-center (*DX* and *AX* center) relaxations for the above four substitutional impurities. In the wz structure there are two nonequivalent *DX* configurations, in which the broken bond (BB) between the impurity and the host atom is either parallel to the *c* axis (DX_1) or along one of the three other equivalent bonds (DX_2). A DX_1 center for oxygen was found to be stable in wz-AlN and metastable in wz-GaN.[59] For silicon, the DX_1 state in wz-AlN has been found to be metastable[59] and both *DX* configurations are unstable in wz-GaN.[60] The DX_2 configuration of C_{Ga} is the ground state in wz-GaN and in wz-AlN in the neutral and negative charge states.[60] Park and Chadi[53] found that Mg and C acceptor impurities in wz-GaN are more stable than the corresponding deep *AX* centers and oxygen is a shallow donor impurity in either cubic or wurtzite-structure GaN, but a DX_1 center is the ground state in wz-AlN. We considered both cases for an oxygen *DX* center on the N site, a silicon *DX* center on an In site, a magnesium *AX* center on an In site, and a carbon *AX* center on a N site and did not find any evidence of off-center relaxations: the impurities return to the ideal substitutional sites without an energy barrier when displaced an appropriate distance (~1.3 Å) away, which shows that these impurities on substitutional sites are the local minimum-energy configuration.

The partial density of states (DOS) show that substitutional oxygen contributes *s*-like states in the conduction band [see Figs. 1(e) and 2(a)] and *p*-like states at the bottom of the valence band [see Fig. 1(e)]. Substitutional silicon introduces *s*-like states at the bottom of the valence band. Moreover, the nearest-neighbor N atoms to Si contribute to the CBM [see Figs. 1(f) and 2(b)]. For the Mg acceptor, the nearest-neighbor N atoms contribute *p*-like states at the top of the valence band [see Figs. 1(g) and 2(c)]. The substitutional carbon atom also contributes *p* states at the top of the valence band [see Figs. 1(h) and 2(d)].

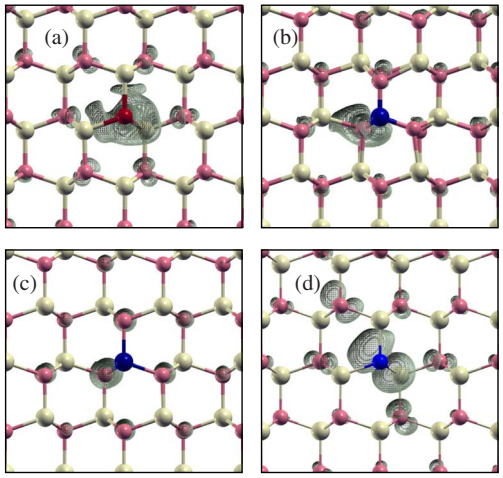

FIG. 2. (Color online) Isosurface plots of the charge density induced by defect states at the Γ point for (a) O_N^+, (b) Si_{In}^+, (c) Mg_{In}^-, and (d) C_N^- in wz-InN. The 0.001 e/Bohr^3 isovalues are shown. Large pale (light yellow) and smaller dark gray (pink) spheres indicate In and N atoms, respectively. The black spheres indicate the impurity atoms.

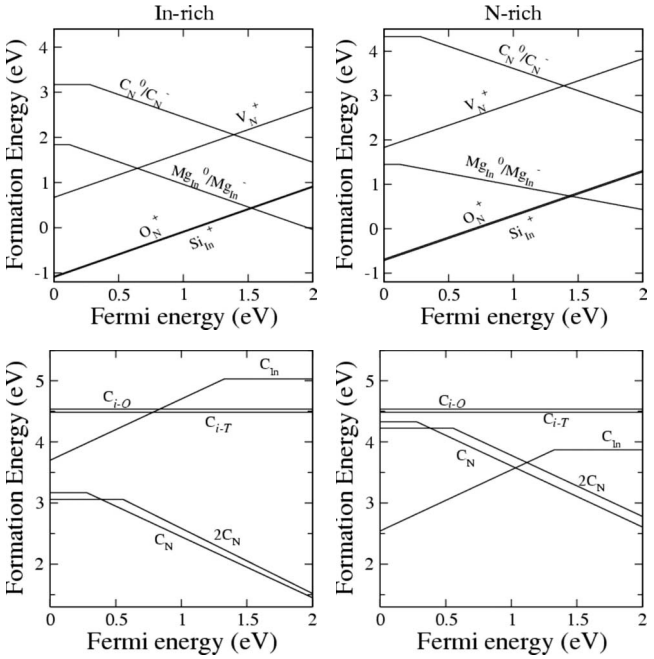

FIG. 3. Formation energies as a function of the Fermi level for impurities and dopants in wz-InN under In-rich (left) and N-rich (right) conditions. The upper panels show single O, Si, Mg, and C impurities and the lower panels give the formation energies for carbon related defects.

We also investigate the interaction between two O (Si, Mg, and C) atoms in InN and find two O, Si, and Mg atoms prefer to be well separated in the neutral state and in the charged states, thus exhibiting a mutually repulsive interaction. Two C atoms in the neutral state, however, prefer to be located on neighboring anion sites in the same (0001) plane and to be separated in the charged state. The binding energy of the two carbon atoms in the neutral charge state is calculated to be 0.11 eV per C atom, and the formation energy per C atom is 3.06 eV and 4.22 eV under In-rich and N-rich conditions, respectively. This defect induces two fully occupied singlet defect states (one below and the other at the VBM) and an unoccupied defect state in the band gap. We find the binding energy in the 2− charge state is −0.07 eV (unbound), so two carbon atoms in this state are unfavorable compared to the isolated C acceptor. In the neutral charge state, we find the formation energies of C_{In}-C_N nearest-neighbor pairs, in parallel and perpendicular configurations, are 6.18 and 6.05 eV under both In- and N-rich conditions and, respectively, their binding energies are 0.97 and 1.10 eV. [We use a "parallel" configuration (∥) indicating one defect is located next to the other and orientated more along the *c* axis. A "perpendicular" configuration (⊥) indicates one defect is located next to the other and orientated more "perpendicular" to the *c* axis.] Thus, the C_{In}-C_N pair exhibits a mutually attractive interaction, and the perpendicular configuration is slightly more stable than the parallel configuration. The neutral C_{In}-C_N complex in the perpendicular configuration induces two fully occupied singlet defect states: one at and one below the VBM and one unoccupied defect state above the CBM. Similarly, for the neutral C_{Ga}-C_N pair in wz-GaN, Wright[28] has found that the formation energy of the pair in the perpendicular direction (4.81 eV) is marginally lower than that of the pair in the parallel orientation (4.96 eV). Boguslawski and Bernholc[60] reported that the C_{Ga}-C_N pair in wz-GaN and the C_{Al}-C_N pair in wz-AlN oriented along the *c* axis are favorable compared to the isolated C dopants.

In Fig. 3 we present the calculated formation energies for substitutional O, Si, Mg, and C atoms (upper panel) and C related defects (lower panel), as a function of Fermi level E_F under In-rich (left) and N-rich (right) conditions. The zero of the Fermi level is chosen at the valence-band maximum. We also include the formation energy for the nitrogen vacancy V_N in the upper panels for comparison.[61] For clarity, for each charge state of each defect, we only show the section of the line with the lowest energy. For the V_N, Si_{In}, and O_N defects, we do not show the neutral charge state since in the DFT calculations, the electron associated with the defect is at the CBM, not in the defect level, thus giving a somewhat artificially low formation energy. Under *p*-type conditions, the formation energies of O_N and Si_{In} in the positive charge state are very low (and nearly equal), which is consistent with the previous study of O_N and Si_{In} in zb-InN.[6] The present result for the O donor is consistent with MOVPE results,[16] where it was reported that the most probable donor is oxygen. The magnesium acceptor has a lower formation energy than the C acceptor and also a lower ionization energy. Thus the results do not indicate any advantages by doping with C. Substitutional carbon on the In site is a donor but has a higher formation energy than the O and Si donors. The present results for C_N and C_{In} in wz-InN behave analogously to carbon in wz-GaN.[28]

We note that there will be some uncertainty in the position of the defect-(and complex) induced states due to the DFT LDA approach, although we expect the qualitative behavior to be captured as was found from self-interaction and relaxation-correction (SIRC) calculations for native point de-

fects in zb-InN.[6] In particular, for O_N^+, Si_{In}^+, and V_N^+ where the conduction-band-related defect state is unoccupied, we can expect the resulting formation energy not to be affected by the value of the band gap (similarly for the MgO_n^{n-1} complexes discussed below). Also for Mg_{In}, the defect-induced state couples to bulk states of the VBM and hence it could be expected to be "tied" to the VBM and not depend significantly on the band-gap value (and similarly for the $Mg_n^{1-n}O$ complexes discussed below). For a more quantitative picture, methods which yield a more accurate description of the band gap, such as *GW*, exact exchange, or SIC, would be valuable.

C. Complexes

The idea of "codoping"[62] is that both acceptors and donors are doped at the same time into a semiconductor and form metastable acceptor-donor-acceptor (A-D-A) complexes for obtaining *p*-type material or donor-acceptor-donor (D-A-D) complexes for obtaining *n*-type material. The formation of A-D-A or D-A-D complexes may be able to enhance the dopant solubility by lowering the formation energy through attractive interactions between the constituents of the defect complex and lower as well the defect transition energy levels through the coupling of donor-acceptor states. First-principles electronic structure calculations and experiments have applied the codoping approach to address *p*-type GaN and AlN (Ref. 62) where the results are promising. (It should be noted however that in the calculations of Ref. 62, the atomic positions were not relaxed and no formation energies or binding energies of the defect complexes were reported nor charge states considered.) Codoping of GaN with magnesium and oxygen has been reported to result in high hole conductivities.[63,64] Yamamoto and Katayama-Yoshida[65] proposed that the complex Mg_{Ga}-O_N-Mg_{Ga} could be effective in enhancing the *p*-type doping efficiency of GaN. A more recent first-principles study has shown that the codoping of the CdTe system may increase the dopant concentration, but it fails to reduce the defect transition energy levels because the donor and acceptor levels have different wave-function characters and symmetry; thus, the level repulsion between them is very weak.[66] In order to produce simultaneously stable bonds and low doping enthalpy (high dopant solubility), a cluster-doping approach, using two species from group-III atoms (Al, Ga, and In) and group-V atoms (N, P, and As) for doping *p*-type ZnO, has been suggested to promote a locally stable chemical environment.[67] To overcome the long-standing "asymmetry doping problem" (i.e., a material can be easily doped either *p*-type or *n*-type, but not both) for the wide band-gap semiconductors, recently, Yan *et al.*[68] proposed an approach where by first doping the host by passive donor-acceptor (D+A) complexes is carried out, which creates fully occupied (unoccupied) impurity bands above (below) the VBM (CBM) of the host. Subsequently, further doping of excess dopant atoms will bind to the (D+A) complexes and effectively dope the fully occupied (unoccupied) impurity bands, which leads to a lower ionization energy. With this approach, the experimental observations of B and H codoped *n*-type diamond[69] and Ga and N codoped *p*-type ZnO (Refs. 70 and 71) were explained.

TABLE III. Formation E^f and binding energies E_b (in eV) of defect complexes. The binding energies of $(MgV_N)^0$ are computed with respect to Mg_{In}^- and V_N^+ and the binding energies of O_NV_{In} in the 0, 1−, and 2− charge states are computed with respect to O_N^+ and V_{In} in the charge states 1−, 2−, and 3−, respectively. The binding energies of $3O_NV_{In}$ in the 0 and 1+ charged states are calculated with respect to O_N^+ and V_{In} in charge states 3− and 2−, respectively. "∥" and "⊥" indicate the parallel and perpendicular configurations, respectively, as explained in the text. "Planar" indicates that the three O atoms are in the (0001) plane.

Defect	Configuration	E^f (In-rich)	E^f (N-rich)	E_b
$(MgV_N)^0$	⊥	1.82	2.60	0.81
	∥	1.76	2.54	0.87
$(O_NV_{In})^0$	⊥	7.30	6.52	0.89
$(O_NV_{In})^0$	∥	7.26	6.49	0.93
$(O_NV_{In})^-$	∥	$7.46-E_F$	$6.68-E_F$	1.48
$(O_NV_{In})^{2-}$	∥	$8.61-2E_F$	$7.84-2E_F$	1.56
$(3O_NV_{In})^0$	3O planar	4.027	4.027	3.99
$(3O_NV_{In})^+$	3O planar	$3.73+E_F$	$3.73+E_F$	3.06
$(3O_NV_{In})^-$	3O planar	$5.63-E_F$	$5.63+E_F$	

With the aim of exploring the codoping or cluster doping approach in InN for achieving *n*- and *p*-type conductivities, we study many possible configurations involving Mg_{In} and O_N, and of Si_{In} and C_N, and also complexes involving vacancies in InN, in particular configurations involving O_NV_{In} and $Mg_{In}V_N$. For each complex in which we identify "clustering," i.e., an attractive interaction between the point defects, we consider the complex in both parallel and perpendicular configurations. In Tables III–V, we list the calculated formation and binding energies of all the defect complexes considered, which are discussed below.

1. Complexes with vacancies

The complex $Mg_{Ga}V_N$ in wz-GaN has been investigated using DFT-GGA calculations. Under Ga-rich conditions, in the neutral charge state, the formation energies in the parallel and perpendicular configurations are 1.37 and 1.33 eV, respectively.[72] The corresponding binding energies with respect to Mg_{Ga}^- and V_N^+ are 0.42 and 0.46 eV, which indicates that V_N prefers to be bound to Mg_{Ga}.[72] We find that the defects Mg_{In} and V_N in wz-InN prefer to be located close together, where the associated binding energies for the neutral parallel and perpendicular structures are 0.87 and 0.81 eV, respectively (relative to Mg_{In}^- and V_N^+). The presence of nitrogen vacancies in GaN and InN therefore indicates *p*-type doping with Mg. The corresponding formation energies under In-rich conditions are 1.76 and 1.82 eV. In the neutral charge state, there are no defect-induced states in the band gap, but there are three unoccupied states at and above the CBM. In the neutral state, the neighboring atoms around the complex relax significantly as shown in Fig. 4 (left panel). Specifically, the bond lengths of Mg and N for the parallel configuration are 2.01 Å, which are 5.6% shorter than the average bond length (2.13 Å) of crystalline Mg_3N_2, and 6.6% shorter than the N-In bond length. The distance

TABLE IV. The formation E^f and binding energies E_b in eV of defect complexes. All the binding energies are computed with respect to Mg_{In}^- and O_N^+. "ac" and "zz" indicate the "armchair" (parallel) and "zigzag" (perpendicular) configurations, respectively (see text).

Defect	Configuration	E^f (In-rich)	E^f (N-rich)	E^f (In-rich): $\mu_{Mg}=E_{Mg}$ (bulk)	E^f (N-rich): $\mu_{Mg}=E_{Mg}$ (bulk)	E_b
$(O_N)^0$		0.47	0.86	0.47	0.86	
$(O_N)^+$		$-1.08+E_F$	$-0.69+E_F$	$-1.08+E_F$	$-0.69+E_F$	
$(Mg_{In})^0$		1.84	1.45	1.64	0.48	
$(Mg_{In})^-$		$1.96-E_F$	$1.57-E_F$	$1.76-E_F$	$0.6-E_F$	
$(MgO)^0$	zz	0.46	0.46	0.26	−0.51	0.43
	ac	0.46	0.46	0.26	−0.51	0.43
$(Mg_2O_2)^0$	zz	0.65	0.65	0.25	−1.29	1.12
	ac	0.652	0.652	0.252	−1.29	1.12
$(Mg_3O_3)^0$	zz	0.88	0.87	0.28	−2.04	1.78
	ac	0.65	0.64	0.05	−2.27	2.01
$(MgO_2)^+$	zz	$-0.85+E_F$	$-0.47+E_F$	$-1.05+E_F$	$-1.44+E_F$	0.66
	ac	$-0.87+E_F$	$-0.49+E_F$	$-1.07+E_F$	$-1.46+E_F$	0.68
$(MgO_3)^{2+}$	zz	$-2.02+2E_F$	$-1.25+2E_F$	$-2.22+2E_F$	$-2.22+2E_F$	0.76
	ac	$-2.03+2E_F$	$-1.26+2E_F$	$-2.23+2E_F$	$-2.23+2E_F$	0.77
$(MgO_4)^{3+}$		$-3.04+3E_F$	$-1.88+3E_F$	$-3.24+3E_F$	$-2.85+3E_F$	0.70
$(Mg_2O)^-$	zz	$2.05-E_F$	$1.66-E_F$	$1.66-E_F$	$-0.28-E_F$	0.79
	ac	$2.03-E_F$	$1.64-E_F$	$1.64-E_F$	$-0.3-E_F$	0.81
$(Mg_3O)^{2-}$	zz	$3.81-2E_F$	$3.03-2E_F$	$3.22-2E_F$	$0.12-2E_F$	0.99
	ac	$3.94-2E_F$	$3.16-2E_F$	$3.35-2E_F$	$0.25-2E_F$	0.86
$(Mg_4O)^{3-}$		$5.55-3E_F$	$4.39-3E_F$	$4.76-3E_F$	$0.51-3E_F$	1.21
$(Mg_2O_3)^+$	zz	$-0.68+E_F$	$-0.30+E_F$	$-1.08+E_F$	$-1.24+E_F$	1.38
	ac	$-0.79+E_F$	$-0.41+E_F$	$-1.19+E_F$	$-2.35+E_F$	1.49
$(Mg_3O_2)^-$	zz	$2.22-E_F$	$1.83-E_F$	$1.62-E_F$	$-1.08-E_F$	1.51
	ac	$2.12-E_F$	$1.73-E_F$	$1.52-E_F$	$-1.18-E_F$	1.61

between Mg and the "ideal" (i.e., bulk) position of the nitrogen vacancy is 15.3% larger than the N-In bond length. For the perpendicular case (Fig. 4, left panel, right figure), the bond lengths between Mg and N are 2.01 and 2.02 Å in the (0001) plane and 2.02 Å along the c axis, where the Mg atom moves away from the ideal position of the nitrogen vacancy by 12%. For both cases, the three In atoms next to V_N move toward the ideal vacancy position by 5% similar to the behavior for isolated V_N.[61]

Motivated by the experimental studies which indicate that V_{In} has a tendency to couple with impurities, such as oxygen,[73] and the *ab initio* investigation which found that the $O_N V_{Ga}$ complex is stable with a large binding energy (~1.8 eV),[20] we investigate the $O_N V_{In}$ complex in wz-InN. We find indeed that the defects O_N and V_{In} like to be located on neighboring sites and $O_N V_{In}$ complex formation is favorable. In the neutral charge state, the binding energies calculated with respect to O_N^+ and V_{In}^- are 0.93 and 0.89 eV, and the formation energies are 7.26 and 7.30 eV under In-rich conditions, for the parallel and perpendicular configurations, respectively (see Table III). We thus focus on the slightly favorable parallel configuration for further investigation. For the defect in the parallel configuration, the average distance between the three planar nearest-neighboring N atoms and the ideal (i.e., bulk) In-vacancy position is 5% larger than the In-N bond length and the oxygen atom moves upward by 10% of the N-In bond length relative to the ideal In-vacancy position. Unlike single O_N, the O-In bond length is 1.1% smaller than the planar N-In distance. The complex induces a doubly occupied singlet defect state just above the VBM and an unoccupied singlet defect state in the gap, thus it can act as an acceptor (see Fig. 5). We therefore consider the 2− and 1− charge states. The atomic structure of this defect complex in the parallel configuration in the 2− charge state is shown in Fig. 6(a). The three planar N atoms nearest to the In vacancy relax inward by 1.9% and the oxygen atom moves away from the ideal N site by 14.3%. The average O-In bond length is 1.6% shorter than the planar N-In distance. The lattice relaxations of the complex $O_N V_{Ga}$ in GaN were reported by Neugebauer and Van de Walle,[20] where the oxygen atom moves away from the ideal Ga vacancy by 14.9%, and the three planar N atoms nearest to the Ga vacancy relax outwards by 9.8% in the 2− charge state. The binding energy of the $O_N V_{In}$ complex increases from ~0.9 eV in the neutral charge state (with respect to O_N^+ and V_{In}^-) to 1.56 eV in the $(O_N V_{In})^{2-}$ charge state relative to O_N^+ and V_{In}^{3-}. The formation energy of this complex is rather high (see Fig. 7) indicating that it will not exist in high concentrations in thermal equilibrium.

TABLE V. The formation E^f and binding energies E_b in eV of defect complexes. The binding energies of SiC are computed with respect to Si_{In}^+ and C_N^-. The binding energies of other complexes (Si_iC and SiC_j, i, and $j \neq 1$) in the neutral state are computed with respect to Si_{In}^0 and C_N^0; in charged states they are computed with respect to Si_{In}^+ and C_N^-. "ac" and "zz" indicate the "armchair" (parallel) and "zigzag" (perpendicular) configurations, respectively (see text).

Defect	Config.	E^f (In-rich)	E^f (N-rich)	E^f(In-rich): $\mu_{Si}=E_{Si}$ (bulk)	E^f (N-rich): $\mu_{Si}=E_{Si}$ (bulk)	E_b
$(Si_{In})^0$		0.33	0.71	−1.30	−2.46	
$(Si_{In})^+$		$-1.10+E_F$	$-0.72+E_F$	$-2.73+E_F$	$-3.89+E_F$	
$(C_N)^0$		3.17	4.33	3.17	4.33	
$(C_N)^-$		$3.45-E_F$	$4.61-E_F$	$3.45-E_F$	$4.61-E_F$	
$(SiC)^0$	zz	1.73	3.28	0.10	0.10	0.61
$(SiC)^0$	ac	1.93	3.48	0.30	0.30	0.41
$(Si_2C)^0$	zz	2.27	4.21	−0.98	−2.14	1.55
$(Si_2C)^+$	zz	$0.82+E_F$	$2.76+E_F$	$-2.43+E_F$	$-3.59+E_F$	0.42
$(Si_3C)^0$	zz	3.42	5.74	−1.47	−3.79	0.73
$(Si_3C)^{2+}$	zz	$0.27+2E_F$	$2.59+2E_F$	$-4.62+2E_F$	$-6.94+2E_F$	−0.13
$(Si_4C)^0$		4.85	7.56	−1.66	−5.14	−0.38
$(Si_4C)^{3+}$		$-0.30+3E_F$	$2.41+3E_F$	$-6.81+3E_F$	$-10.29+3E_F$	−0.67
$(SiC_2)^0$	Zz	4.50	7.21	2.88	4.04	2.16
$(SiC_2)^-$	Zz	$4.83-E_F$	$7.54-E_F$	$3.20-E_F$	$4.36-E_F$	0.96
$(SiC_3)^0$	Zz	7.34	11.21	5.72	8.04	2.49
$(SiC_3)^{2-}$	Zz	$8.18-2E_F$	$12.05-2E_F$	$6.55-2E_F$	$8.87-2E_F$	1.06
$(SiC_4)^0$		10.30	15.33	8.67	12.15	2.70
$(SiC_4)^{3-}$		$11.67-3E_F$	$16.70-3E_F$	$10.04-3E_F$	$13.52-3E_F$	1.02

We also consider a configuration with one indium vacancy, V_{In}, and three planar oxygen atoms $3O_N$, as shown in Fig. 6(b). The formation energy in the neutral charge state significantly decreases compared the $O_N V_{In}$ complex under both In- and N-rich conditions as shown in Fig. 7. The neutral defect induces three fully occupied singlet defect states: one in the band gap and the other two at the top of the valence band, and an unoccupied defect state at the CBM [see Fig. 5 (right)]. We consider 3+, 2+, 1+, 1−, and 2− charge states and find the 3+, 2+, and 2− charge states are unstable. The 1+ charge state is stable in a small energy window ($E_F < 0.3$ eV). We therefore do not consider further positive charge states. In the neutral charge state, the three oxygen atoms relax outward from the ideal N sites, away from the In vacancy by 10% of the In-N bond length, and the distance between each oxygen atom and its nearest-neighbor In atom is contracted by 1.2% relative to the ideal N-In bond length. In the 1− and 1+ charge states, the O-In distances are very similar to those in the neutral charge state, namely, the oxygen atoms move outward from the ideal N sites by 9.8% and 8% of the bulk N-In bond length, respectively.

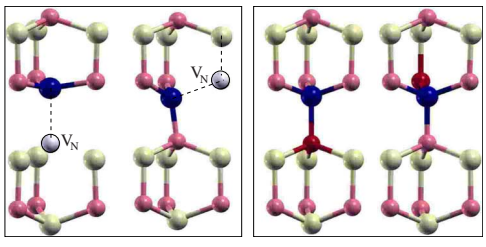

FIG. 4. (Color online) Left panel: "parallel" (left) and "perpendicular" (right) atomic geometries of the neutral ($Mg_{In}V_N$) complex. Right panel: the neutral $Mg_{In}O_N$ defect for the "parallel" (left) and "perpendicular" (right) configurations, in wz-InN. Large pale (light yellow) and smaller darker gray (pink) spheres indicate In and N atoms, respectively. Large and small black (blue and red) spheres indicate Mg and O atoms, respectively. The vacancies are indicated by the circled pale spheres. Only the neighboring atoms of the complexes are shown for clarity.

2. Mg_mO_n *complexes*

We investigate the interaction between Mg_{In} and O_N and find that they prefer to be located on nearest-neighbor sites, where the binding energy is 0.43 eV, relative to the single defects Mg_{In}^- and O_N^+. The total energy of the configuration with Mg_{In} and O_N far apart is 0.45 eV higher. For both per-

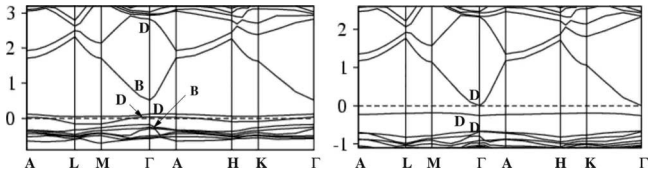

FIG. 5. Band structures for the $V_{In}O_N$ (left) and $3O_N V_{In}$ (right) defect complexes in the neutral charge state in wz-InN. The labels "B" and "D" represent bulk and defect states, respectively. The horizontal dotted lines are the Fermi levels.

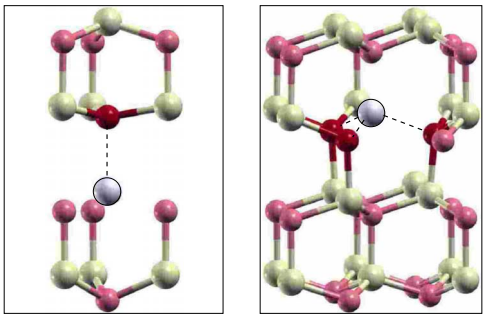

FIG. 6. (Color online) Atomic geometry of the (a) $(O_N V_{In})^{2-}$ and (b) $3O_N V_{In}$ defect complexes. Large pale (light yellow) and smaller darker gray (pink) spheres indicate In and N atoms, respectively. Small black (red) spheres and pale circled spheres indicate O atoms and vacancies, respectively. Only the neighboring atoms of the complexes are shown for clarity.

pendicular and parallel configurations, the total energies are identical as indicated in Table IV, and the relaxed Mg-O bond lengths are close to that of crystalline MgO, where the bond length is 2.10 Å. The atomic structures of the MgO complexes are shown in Fig. 4 (right). As discussed above, Mg_{In} is an acceptor and O_N is a donor. In forming the $Mg_{In}O_N$ defect, we find that there are no longer any states in the band gap, but there is a doubly occupied singlet defect state at the VBM [see Fig. 10(a)]. For the Mg_2O_2 complex in the parallel and perpendicular configurations, which form Mg-O armchair and zigzag structures, respectively (see Fig. 8), there is a very tiny energy difference (2 meV). The calculated binding energy of 1.12 eV shows that the defects still like to be located close to each other. In particular, per MgO unit, the binding energy is 0.56 eV, which is larger than the single MgO complex (0.43 eV), showing it is favorable to form the larger cluster of Mg_2O_2. This defect induces a fully occupied state at the VBM, and an unoccupied defect state above the CBM. We also consider a larger complex, Mg_3O_3. Here we used a 128-atom cell to avoid interactions between the complexes in neighboring cells. We find that the armchair structure is more stable than the zigzag structure by 0.23 eV. The binding energy of the armchair complex is 2.01 eV (see Table IV) or 0.67 eV per MgO pair, indicating that clustering is favorable. Correspondingly, the formation energies of the

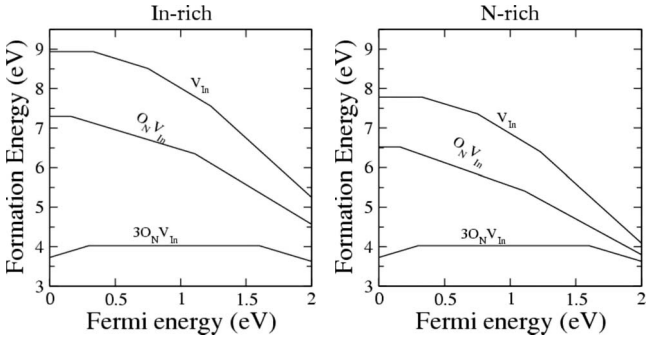

FIG. 7. Formation energies as a function of the Fermi level for impurity complexes involving V_{In} and O_N in wz-InN under In-rich (left) and N-rich (right) conditions.

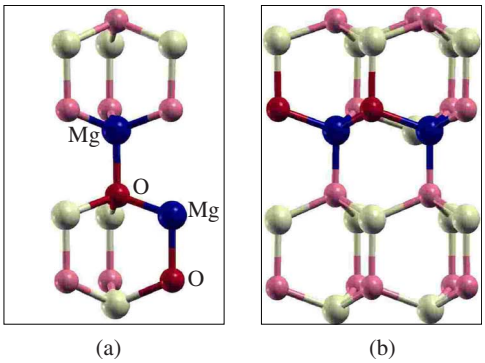

FIG. 8. (Color online) Atomic geometry of the Mg_2O_2 complexes in wz-InN with a (a) "parallel" ("armchair") configuration and a (b) "perpendicular" ("zig-zag") configuration. Large pale (light yellow) and smaller darker gray (pink) spheres indicate In and N atoms, respectively. Large (blue) and small dark gray (red) spheres indicate Mg and O atoms, respectively. Only the neighboring atoms of the complexes are shown for clarity.

MgO, Mg_2O_2, and Mg_3O_3 complexes are 0.46, 0.65, and 0.65 eV, respectively, or 0.46, 0.32, and 0.21 eV per MgO pair. We conclude that these defects could play a role in the compensation of acceptor doping with Mg if oxygen is present as a contaminant. We note that the calculated binding energies are comparable to the values reported of 0.50 and 0.58 eV for parallel and perpendicular MgO in wz-GaN (Ref. 26) and 0.60 eV for MgO and 0.80 eV for Mg_2O_2 in zb-AlN.[19]

In addition to the above-mentioned complexes, we also consider codoping and cluster doping involving Mg acceptors and O donors with regard to varying the relative concentrations of each species. For the complexes Mg_2O, Mg_3O, MgO_2, and MgO_3, we consider both parallel and perpendicu-

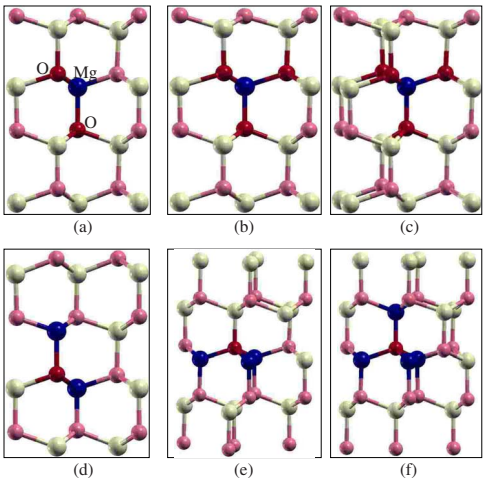

FIG. 9. (Color online) Atomic geometry of the most stable Mg_nO_m defect complexes in wz-InN: (a) "parallel" MgO_2, (b) "parallel" MgO_3, (c) MgO_4; (d) "parallel" Mg_2O, (e) "perpendicular" Mg_3O, and (f) Mg_4O. Large pale (light yellow) and smaller darker gray (pink) spheres indicate In and N atoms, respectively. Large (blue) and small dark gray (red) spheres indicate Mg and O atoms, respectively. Only the neighboring atoms of the impurities are shown for clarity.

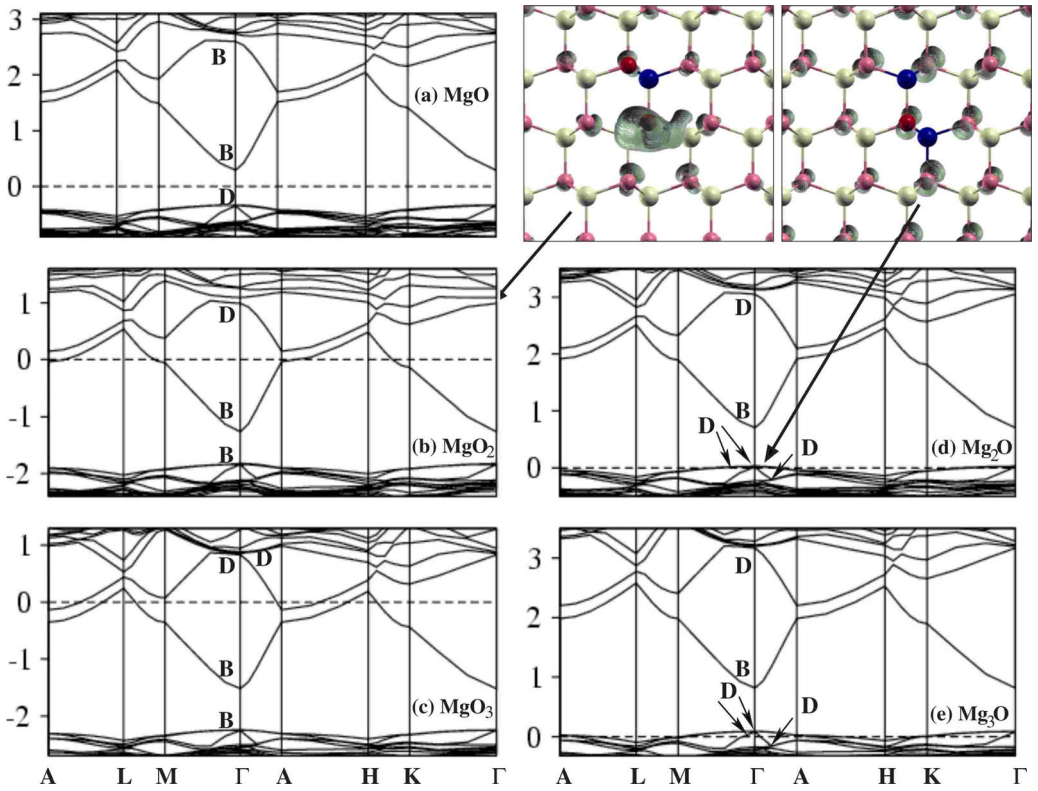

FIG. 10. (Color online) Band structures for the stable Mg_nO_m defect complexes in the neutral charge state in wz-InN. The labels "B" and "D" represent bulk and defect states, respectively. The horizontally dotted lines are the Fermi levels [except for (a) where it is placed in the center of the band-gap]. For Mg_2O and MgO_2, isosurface plots are shown of the charge density induced by the defect states as indicated by the long arrows. The 0.001 e/Bohr^3 isovalues are shown. Large pale (light yellow) and smaller darker gray (pink) spheres indicate In and N atoms, respectively. Large (blue) and small black (red) spheres indicate Mg and O atoms, respectively.

lar configurations in the neutral charge state. For the complexes Mg_4O and MgO_4, we only consider the configurations shown in Figs. 9(c) and 9(f). From examination of the associated electronic structure and occupancies of the induced defect levels, relevant charge states of the (favorable) defect complexes are then considered. Figure 9 shows the atomic geometries of the most stable Mg_mO_n complexes for $m=1$ and $n=2,3$ [see Figs. 9(a) and 9(b)] and $n=1$ and $m=2,3$ [see Figs. 9(d) and 9(e)]. In the neutral charge state, the Mg-O bond lengths, 2.10 and 2.09 Å in Mg_2O and 2.09 and 2.09 Å in MgO_2, are close to that of crystalline MgO (2.10 Å). The average Mg-O bond length is 2.07 and 2.06 Å in the neutral Mg_3O and MgO_3 complexes, respectively. With one more acceptor or donor added to the complexes, resulting in Mg_4O and MgO_4, the average distances between Mg-O become slightly contracted to 2.04 Å for both Mg_4O and MgO_4. The neutral MgO_2 and MgO_3 complexes give rise to unoccupied defect states above the CBM [see Figs. 10(b) and 10(c)]. There are one (MgO_2) and two (MgO_3) electrons associated with these states, which due to the electron filling in the DFT calculations, occupy the CBM instead. Thus, these complexes are donors and we can consider the 1+ and 2+ charge states, respectively. The neutral MgO_4 complex induces two defect states in the conduction band with three associated electrons, thus it acts as a donor. For this complex, we consider charge states 1+, 2+, and 3+. Neutral Mg_2O (Mg_3O) yields a hole (two holes) at (above) the VBM, thus it can act as an acceptor [see Figs. 10(d) and 10(e)]. The neutral Mg_4O complex induces three holes above the VBM. Thus, for these complexes, we consider 1−, 2−, and 3− charge states, respectively. The average Mg-O bond lengths are close to that of crystalline MgO (2.10 Å) in the charged states for all the complexes we considered. The formation (and binding) energies of the parallel and perpendicular configurations in the ionized states for the various complexes are close, as shown in Table IV.

We also consider complexes with more than one donor and acceptor at the same time in 128-atom cell, that is, Mg_2O_3 and Mg_3O_2 in parallel and perpendicular configurations. We find that the parallel configuration is more favorable for both complexes (see Table IV). The neutral Mg_2O_3 complex induces a defect state above the CBM with an associated electron and thus acts as a single donor. The average Mg-O bond length of this complex is 2.08 Å in both the neutral charge state and in the 1+ charge state. The neutral Mg_3O_2 complex induces a hole at the VBM and thus acts as an acceptor. The average Mg-O bond length is 2.09 Å in both the neutral charge state and in the 1− charge state. The ionization energy of the acceptor Mg_2O (Mg_3O_2) decreases to 0.05 eV (0.02 eV) compared to the value 0.12 eV of the isolated Mg acceptor.

Figure 11 shows the calculated formation energies of the Mg_mO_n complexes as a function of the Fermi level for both In-rich (left) and N-rich (right) conditions. Here the zero of

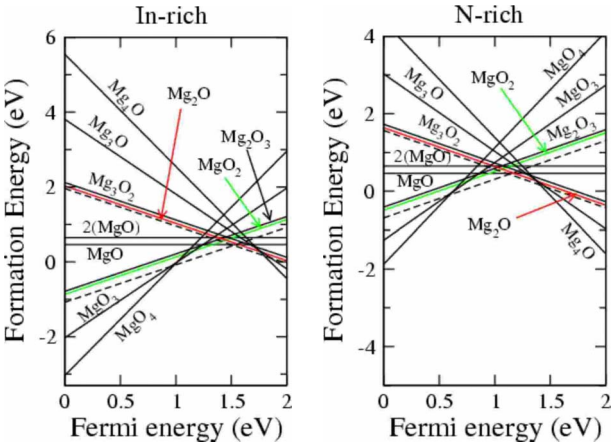

FIG. 11. (Color online) Formation energies as a function of the Fermi level for Mg_mO_n complexes in wz-InN under In-rich (left) and N-rich (right) conditions. The O_N^+ donor and Mg_{In}^- acceptor in dashed lines are included for comparison.

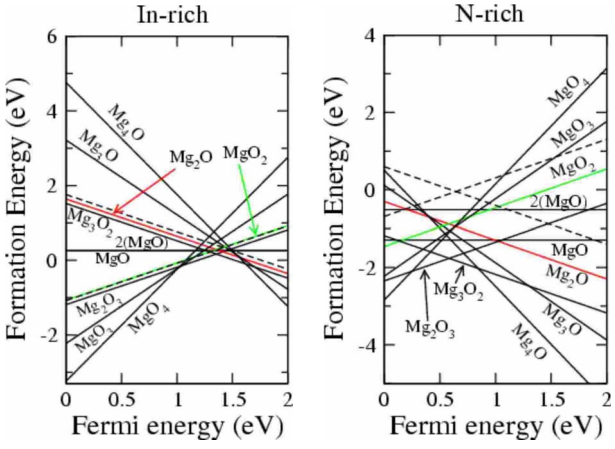

FIG. 12. (Color online) Formation energies as a function of the Fermi level for Mg_nO_m complexes in wz-InN under In-rich (left) and N-rich (right) conditions, where $\mu_{Mg}=E_{Mg}$ (bulk). The O_N^+ donor and Mg_{In}^- acceptor in dashed lines are included for comparison.

the Fermi level is chosen at the VBM. We also include the formation energies of O_N and Mg_{In} for comparison (long-dashed lines in Fig. 11). It is interesting to note that for $n>m$ (of the Mg_mO_n complexes), the formation energies are low in p-type material where the formation energy decreases with the increasing oxygen content. While for $n<m$ (of Mg_mO_n), the formation energies are higher in p type but lower in n-type material, and the formation energy decreases with increasing Mg content in n-type InN and the binding energy slightly increases as well. Another feature worth noting is that the formation energies for MgO_2 and Mg_2O_3 (where $n-m=-1$) are comparable and similarly for Mg_2O and Mg_3O_2 (where $n-m=1$). We therefore predict the Mg_mO_n complexes could be important defects in InN under both In-rich and N-rich conditions and their properties and behavior could be controlled by the Mg and O contents.

We also calculate the formation energies of the defect complexes considering that the Mg solubility is limited by bulk Mg, i.e., by assuming the second phase Mg_3N_2 can be prevented from forming. The results are listed in Table IV and shown in Fig. 12. Here we set $\mu_{Mg}=E_{Mg}$ (bulk) and the atom chemical potentials of N, In, and O are assumed to be determined by thermal equilibrium with InN and In_2O_3, respectively, i.e., for In-rich conditions $\mu_{In}=E_{In}$ (bulk), $\mu_N=E_{InN}-E_{In}$ (bulk), $\mu_{Mg}=E_{Mg}$ (bulk), and $\mu_O=1/3[E_{In_2O_3}-2E_{In}(\text{bulk})]$; for N-rich conditions, $\mu_{In}=E_{InN}-1/2E_{N_2}$, $\mu_N=1/2E_{N_2}$, $\mu_{Mg}=E_{Mg}$ (bulk), and $\mu_O=1/3[E_{In_2O_3}-2(E_{InN}-1/2E_{N_2})]$. It can be seen that in these circumstances, the formation energies of the defect complexes decrease under both In- and N-rich conditions. It is worth noting that under N-rich conditions, the formation energy of the isolated Mg acceptor decreases by ~ 1 eV, which indicates that the efficiency of p-type doping of Mg-doped InN could be improved. As mentioned in Sec. I, recent experiments[13,14] have shown evidence of p-type conductivity in heavily Mg-doped InN. The present results indicate that it could be possible to improve the efficiency by codoping or "cluster doping" of Mg_mO_n complexes and, in particular, by increasing the Mg concentration through the use of bulk Mg as the reservoir for μ_{Mg} then tuning the oxygen concentration to achieve both p- and n-type InN. Interestingly, it has been experimentally reported that p-type doping of GaN could be enhanced by doping with Mg in an oxygen environment.[63,74] Very similar behavior is found when including the In-4d electrons as valence.[75]

3. Si_iC_j complexes

Analogously to the Mg-O acceptor-donor system, we also consider the codoping of Si-C donors and acceptors and compare the behavior of this system to that of Mg-O. Recent experimental investigations have studied Si and C in GaN (Refs. 76–78). The system is likely to be associated with the yellow luminescence in C-doped GaN films and responsible for the semi-insulating behavior of GaN:C:Si films. It was found[76,77] that when carbon concentrations were less than that of silicon, carbon should incorporate as C_N and compensate the Si donors. When C concentrations exceeded that of Si, carbon became the dominant active species and the material became insulating due to self-compensation. However, the interaction between C and Si was not considered. To date there have been no experimental and theoretical studies involving Si and C codoping InN. We therefore investigated possible complex formation between Si_{In} and C_N. We find that they prefer to be located on neighboring sites, where the binding energy is 0.61 eV for the perpendicular configuration and 0.41 eV for the parallel configuration, relative to the single defects Si_{In}^+ and C_N^-. For comparison, the total energy of the configuration with Si_{In} and C_N far apart is 0.49 eV higher than that of the perpendicular configuration. The perpendicular configuration has the lower formation energy 1.73 and 3.28 eV under In- and N-rich rich conditions, respectively, and the parallel structure is 0.2 eV higher. We therefore only study the perpendicular configuration for other Si_iC_j configurations. The SiC complex induces two occupied singlet defect states close to the VBM and no defect state in the gap [see Fig. 14(a)]. The Si-C bond length is 1.85 Å, close to that in bulk α-SiC (1.88 Å in the planar and 1.89 Å in the apical directions).

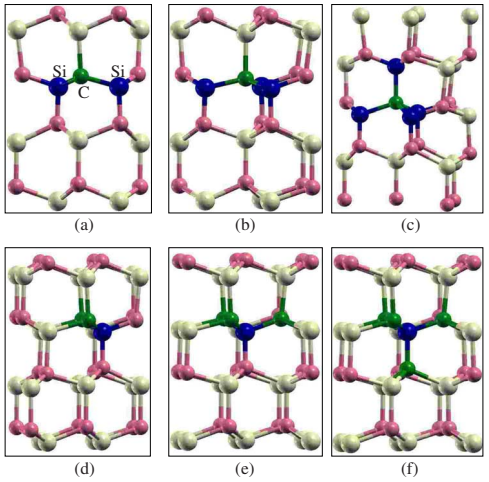

FIG. 13. (Color online) Atomic geometry of the most stable Si_iC_j defect complexes in wz-InN: (a) "zigzag" Si_2C, (b) Si_3C, (c) Si_4C; (d) "zigzag" SiC_2, (e) SiC_3, and (f) SiC_4. Large pale (light yellow) and smaller darker gray (pink) spheres indicate In and N atoms, respectively. Large (blue) and small dark gray (green) spheres indicate Si and C atoms, respectively. Only the neighboring atoms of the impurities are shown for clarity.

Similar to the Mg_mO_n complexes, we consider both parallel and perpendicular configurations for the complexes Si_2C, Si_3C, SiC_2, and SiC_3. Figure 13 shows the relaxed atomic geometries of the most stable Si_iC_j complexes for $i=1$ and $j=2,3$ [see Figs. 13(a) and 13(b)] and $j=1$ and $i=2,3$ [see Figs. 13(d) and 13(e)]. For the complexes Si_4C and SiC_4, the configurations shown in Figs. 13(c) and 13(f) are considered. (Here we have dropped the subscript indicating which site the impurities occupy with the understanding that Si occupies the In site and C is on a N site.) The average Si-C bond length is 1.86 Å for SiC_2, 1.88 Å for SiC_3, and 1.89 Å for SiC_4 complexes. The corresponding values are 1.94, 2.04, and 2.10 Å for the Si_2C, Si_3C, and Si_4C complexes, respectively. The complexes Si_2C and Si_3C have larger binding energies than the SiC complex in the neutral charge states (as listed in Table V). The complex Si_2C induces a singlet defect state occupied with one electron in the conduction band and the complex Si_3C induces a fully occupied singlet defect state in the conduction band [see Figs. 14(b) and 14(c)]. As for the Mg_mO_n complexes ($m=1$ and $n=2$ and 3), these electrons are located at the CBM and not in the defect level due to the electron filling in the DFT calculations. These Si_2C and Si_3C complexes are therefore donors. We investigate the relevant positive charge states and find that the attractive interaction among the impurities in Si_2C is weaker than the neutral case (compare 0.42 to 1.55 eV). For the Si_3C complex in the 2+ charge state, the interaction is slightly repulsive (−0.13 eV), which implies that this complex would change to other configurations over time if the two electrons are removed. The binding energy of the Si_4C complex is negative (−0.38 eV), i.e., repulsive, in the

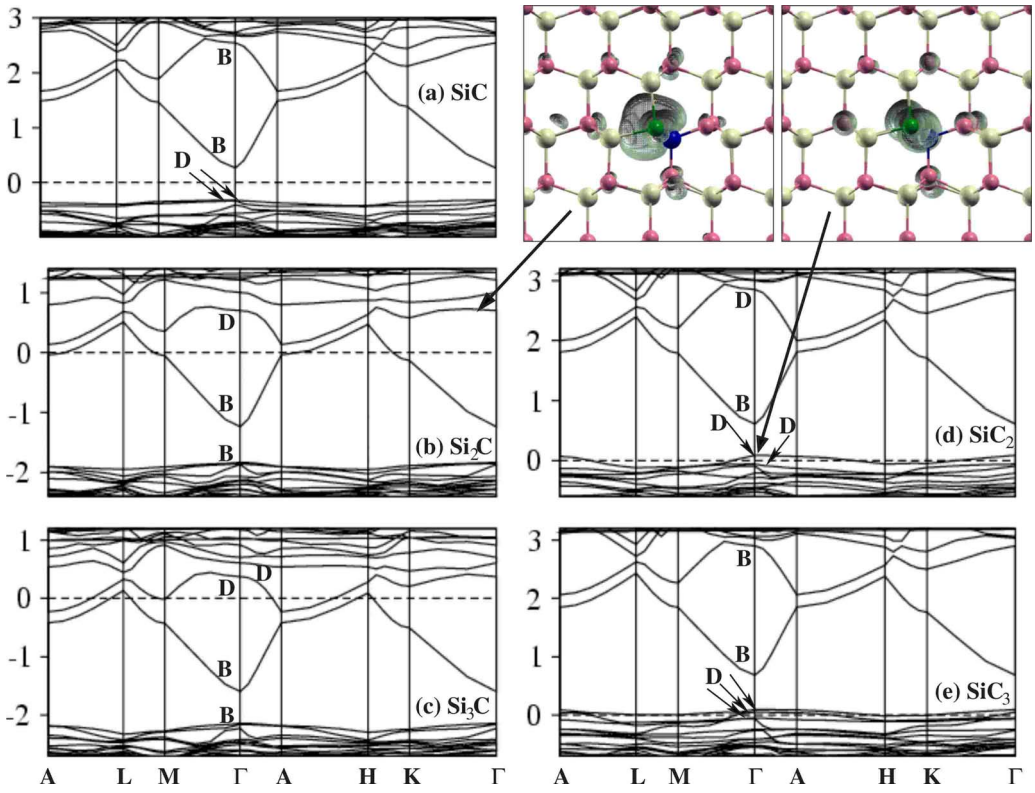

FIG. 14. (Color online) Band structures for Si_iC_j defect complexes in the neutral state in wz-InN. The labels "B" and "D" represent bulk and defect states, respectively. The horizontally dotted lines are the Fermi levels [except for (a) where it is placed in the center of the band-gap]. For Si_2C and SiC_2, isosurface plots of the charge density induced by the defect states are indicated by the long arrows. The 0.001 e/Bohr^3 isovalues are shown. Large pale (light yellow) and smaller darker gray (pink) spheres indicate In and N atoms, respectively. Large (blue) and small black (green) spheres indicate Si and C atoms, respectively.

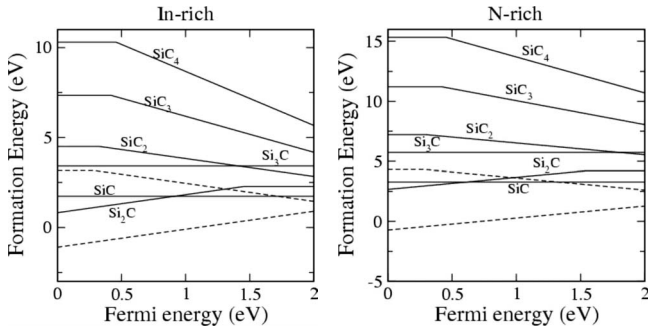

FIG. 15. Formation energies as a function of the Fermi level for Si_iC_j complexes in wz-InN under In-rich (left) and N-rich (right) conditions. The Si_{In}^{+} donor and C_N^{-} acceptor (dashed lines) are included for comparison.

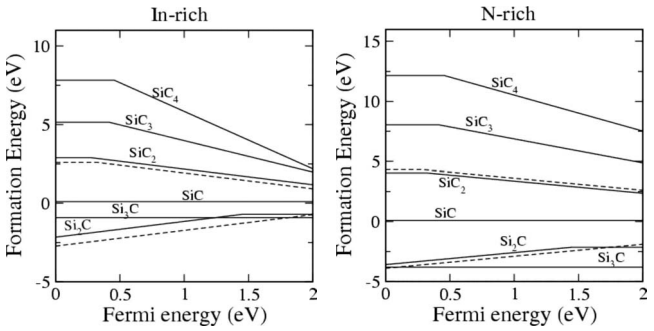

FIG. 16. Formation energies as a function of the Fermi level for Si_iC_j complexes in wz-InN under In-rich (left) and N-rich (right) conditions, where $\mu_{Si}=E_{Si}$ (bulk). The Si_{In}^{+} donor and C_N^{-} acceptor (dashed lines) are included for comparison.

neutral charge state, and it induces two defect states (one with two electrons and the other with one electron) in the conduction band. The interactions among the impurities are still repulsive in the 3+ charge state, which indicates that this complex cannot exist in either the neutral or the 3+ charge states. (Note, we did not consider the 1+ and 2+ charge states.)

The complexes SiC_j ($j=2-4$) have large binding energies in the neutral charge states, and the binding energy increases with increasing C in the complex (from 2.16 to 2.70 eV) (as listed in Table V). The complexes SiC_2 and SiC_3 induce a hole at the VBM and two holes above the top of the valence band, respectively [see Figs. 14(d) and 14(e)]. For the relevant negative charge states (1− for SiC_2 and 1− and 2− for SiC_3), the attractive interactions among the impurities become weaker than for the neutral cases, but they are still mutually attractive. The SiC_4 complex induces three holes close to the VBM and in the 3− charge state, the binding energy is ~1 eV similar to $(SiC_2)^{-}$ and $(SiC_3)^{2-}$.

The formation and binding energies are listed in Table V, where the former are given under In- and N-rich conditions. Figure 15 shows the calculated formation energies of the Si_iC_j defect complexes as a function of Fermi level, E_F, for both In-rich (left) and N-rich (right) conditions. Here the zero of Fermi level is chosen at the valence-band maximum. For comparison we include the result for the single Si and C impurities. Under In-rich conditions, for the complexes with $i<j$, the formation energies are all higher than 2.5 eV; thus these defect complexes can hardly exist in significant concentration in thermal equilibrium, although the clusters have large binding energies. Under N-rich conditions, the formation energies of the complexes are even higher. It can be furthermore seen that these complexes do not suggest any doping advantage over isolated Si atoms.

We also considered the formation energy assuming the silicon atom chemical potential is from bulk Si, i.e., $\mu_{Si}=E_{Si}$ (bulk) and the carbon chemical potential μ_C is taken as the total-energy per carbon atom in the graphite structure. The atom chemical potentials of N and In are assumed to be determined by thermal equilibrium with InN, i.e., for In-rich conditions, $\mu_{In}=E_{In}$ (bulk) and $\mu_N=E_{InN}-E_{In}$ (bulk) and for N-rich conditions, $\mu_{In}=E_{InN}-1/2E_{N_2}$ and $\mu_N=1/2E_{N_2}$. The formation energies (as listed in Table V and shown in Fig. 16) for all the defect complexes decrease as compared to the corresponding values obtained assuming the solubility limit for Si is determined by Si_3N_4, as described above. The complexes with $i\geq j$ have very low formation energies (<0.1 eV) under both In- and N-rich conditions. The formation energy of the SiC_2 complex is only marginally less favorable than isolated C, but the C acceptor is in any case not a better p-type dopant than the Mg acceptor. With regard to obtaining n-type doping, still none of the Si_iN_j complexes investigated indicates any advantage over isolated Si_{In}. We find similar behavior when including the In-4d electrons as valence.[79]

IV. CONCLUSIONS

We have calculated systematically the structural and electronic properties, and formation energies, of various impurities (O, Si, Mg, and C) and their complexes in wurtzite InN, which might be intentionally or unintentionally introduced during growth of the material. We show that substitutional O and Si act as single donors and substitutional C and Mg act as single acceptors. The Mg acceptor has a lower formation energy than the C acceptor; thus it is the more favorable acceptor under both In- and N-rich conditions. The interaction between two O, Si, and Mg atoms is predicted to be mutually repulsive in both the neutral and ionized states. While two carbon atoms exhibit an attractive interaction in the neutral charge states, they become repulsive in their ionized states. The nitrogen vacancy, V_N, prefers to be bound to Mg_{In}, forming a $Mg_{In}V_N$ complex in thermal equilibrium; similar behavior has been found for V_N and Mg_{Ga} in wz-GaN.[72] The O_NV_{In} complex has a high formation energy even though V_{In} has a tendency to bind with oxygen. The formation energy of the $3O_NV_{In}$ complex is significantly lower, but still too high to be an important defect in InN. We predict the Mg_mO_n complexes could be important defects in InN under both In-rich and N-rich conditions for obtaining improved efficiency for n- and p-type conductivities through tuning of the relative concentrations of Mg and O; in particular, by providing the maximum Mg solubility through the use of the chemical potential of Mg from bulk Mg. Complexes based on codoping of Si and C appear to offer no advantage in obtaining n- or p-type conductivity over isolated dopants.

ACKNOWLEDGMENTS

We gratefully acknowledge support from the Australian Research Council (ARC) and computer resources from the Australian Partnership for Advanced Computing (APAC) National Facility and the Australian Centre for Advanced Computing and Communications.

[1] A. G. Bhuiyan, A. Hashimoto, and A. Yamamoto, J. Appl. Phys. **94**, 2779 (2003).
[2] K. S. A. Butcher and T. L. Tansley, Superlattices Microstruct. **38**, 1 (2005).
[3] W. Walukiewicz, J. W. Ager III, K. M. Yu, Z. Liliental-Weber, J. Wu, S. X. Li, R. E. Jones, and J. D. Denlinger, J. Phys. D **39**, R83 (2006).
[4] S. N. Mohammad and H. Morkoc, Prog. Quantum Electron. **20**, 361 (1996).
[5] B. E. Foutz, S. K. O'Leary, M. S. Shur, and L. F. Eastman, J. Appl. Phys. **85**, 7727 (1999).
[6] C. Stampfl, C. G. Van de Walle, D. Vogel, P. Krüger, and J. Pollmann, Phys. Rev. B **61**, R7846 (2000).
[7] A. Qteish, A. I. Al-Sharif, M. Fuchs, M. Scheffler, S. Boeck, and J. Neugebauer, Phys. Rev. B **72**, 155317 (2005).
[8] P. Rinke, M. Scheffler, A. Qteish, M. Winkelnkemper, D. Bimberg, and J. Neugebauer, Appl. Phys. Lett. **89**, 161919 (2006).
[9] S. H. Wei and A. Zunger, Phys. Rev. B **37**, 8958 (1988).
[10] D. W. Jenkins and J. D. Dow, Phys. Rev. B **39**, 3317 (1989).
[11] P. Specht, R. Armitage, J. Ho, E. Gunawan, Q. Yang, X. Xu, C. Kisielowski, and E. R. Weber, J. Cryst. Growth **269**, 111 (2004).
[12] X. Wang, S.-B. Che, Y. Ishitani, and A. Yoshikawa, Appl. Phys. Lett. **91**, 081912 (2007).
[13] R. E. Jones, K. M. Yu, S. X. Li, W. Walukiewicz, J. W. Ager, E. E. Haller, H. Lu, and W. J. Schaff, Phys. Rev. Lett. **96**, 125505 (2006).
[14] P. A. Anderson, C. H. Swartz, D. Carder, R. J. Reeves, S. M. Durbin, S. Chandril, and T. H. Myers, Appl. Phys. Lett. **89**, 184104 (2006).
[15] T. L. Tansley and R. J. Egan, Phys. Rev. B **45**, 10942 (1992); *Wide Band Gap Semiconductors*, MRS Symposia Proceedings No. 242 (Materials Research Society, Pittsburgh, 1992), p. 395.
[16] A. Yamamoto, H. Miwa, Y. Shibata, and A. Hashimato, Thin Solid Films **494**, 74 (2006).
[17] S. Nakamura, M. Senoh, S. Nagahama, N. Iwasa, T. Yamada, T. Matsushita, Y. Sugimoto, and H. Kiyoku, Appl. Phys. Lett. **70**, 1417 (1997).
[18] K. Zhu, M. L. Nakarmi, K. H. Kim, J. Y. Lin, and H. X. Jiang, Appl. Phys. Lett. **85**, 4669 (2004).
[19] C. Stampfl and C. G. Van de Walle, Phys. Rev. B **65**, 155212 (2002).
[20] J. Neugebauer and C. G. Van de Walle, Appl. Phys. Lett. **69**, 503 (1996).
[21] H. Timmers, K. Scott, A. Butcher, S. K. Shrestha, P. P. T. Chen, M. Wintrebert-Fouquet, and R. Dogra, J. Cryst. Growth **288**, 236 (2006).
[22] C. G. Van de Walle, C. Stampfl, and J. Neugebauer, J. Cryst. Growth **189-190**, 505 (1998).
[23] R. Q. Wu, L. Shen, M. Yang, Z. D. Sha, Y. Q. Cai, Y. P. Feng, Z. G. Huang, and Q. Y. Wu, Phys. Rev. B **77**, 073203 (2008).
[24] I. Gorczyca, A. Svane, and N. E. Christensen, Phys. Rev. B **61**, 7494 (2000).
[25] T. Mattila and R. M. Nieminen, Phys. Rev. B **55**, 9571 (1997).
[26] A. F. Wright, J. Appl. Phys. **98**, 103531 (2005).
[27] P. Boguslawski, E. L. Briggs, and J. Bernholc, Appl. Phys. Lett. **69**, 233 (1996).
[28] A. F. Wright, J. Appl. Phys. **92**, 2575 (2002).
[29] S. Baroni, A. Dal Corso, S. de Gironcoli, and P. Giannozzi (http://www.pwscf.org).
[30] S. G. Louie, S. Froyen, and M. L. Cohen, Phys. Rev. B **26**, 1738 (1982).
[31] The norm-conserving pseudopotential for In was generated with a scalar-relativistic calculation by P. Giannozzi and X. Gonze *et al.* based on the one generated by X. Gonze, R. Stumpf, and M. Scheffler [Phys. Rev. B **44**, 8503 (1991), and references cited therein], but with core correction added.
[32] *Properties of Group-III Nitrides*, edited by J. H. Edgar, EMIS Datareviews Series (IEE, London, 1994).
[33] M. Fuchs, J. L. F. Da Silva, C. Stampfl, J. Neugebauer, and M. Scheffler, Phys. Rev. B **65**, 245212 (2002).
[34] J. Wu, W. Walukiewicz, K. M. Yu, J. W. Ager III, E. E. Haller, H. Lu, W. J. Schaff, Y. Saito, and Y. Nanishi, Appl. Phys. Lett. **80**, 3967 (2002).
[35] T. V. Shubina, S. V. Ivanov, V. N. Jmerik, D. D. Solnyshkov, V. A. Vekshin, P. S. Kop'ev, A. Vasson, J. Leymarie, A. Kavokin, H. Amano, K. Shimono, A. Kasic, and B. Monemar, Phys. Rev. Lett. **92**, 117407 (2004).
[36] *Ab initio* calculations in the literature give a wide range of values for the band gap of wurtzite InN depending on the description: all-electron and pesudopotential calculations including the In 4*d* electrons yield a tiny, no, or negative band gap (Refs. 80 and 81), self-interaction and relaxation corrected pseudopotential calculations give 1.55 eV (Ref. 6), *GW* calculations yield 0.02 eV (Ref. 81), and using the exact-exchange (EXX) approach (Ref. 7), a value of ~1.4 eV was estimated. More recent first-principles calculations including quasiparticle effects (in combination with other treatments, e.g., self-interaction correction, EXX) report band gaps closer to 0.7–0.8 eV (Ref. 8). With the present nonlinear core correction approach, the band gap is calculated to be 0.65 eV, larger than the value of 0.0 eV with the In 4*d* electrons included in the pesudopotential calculations. We note that it is usual for the nlcc approach to yield a somewhat larger gap than treatments which include the Indium 4*d* electrons. This is due to the absence of repulsion between the metal *d* states and the top valence *p* states, of the anion atom, at the zone center (see, e.g., the discussion in Ref. 9).
[37] C. G. Van de Walle and J. Neugebauer, J. Appl. Phys. **95**, 3851 (2004).
[38] We use the DMol^3 code. B. Delley, J. Chem. Phys. **113**, 7756 (2000); **92**, 508 (1990). With an atomic cut-off radius of 9 Bohr to calculate the bulk properties of In_2O_3 and Mg_3N_2, using a $2\times2\times2$ **k**-point mesh, β-Si_3N_4 using a $2\times2\times6$ **k**-point mesh, and MgO and SiC using an $8\times8\times8$ **k**-point mesh and an atomic cut-off radius of 11 Bohr.

[39] K. L. Chopra, S. Major, and D. K. Pandya, Thin Solid Films **102**, 1 (1983).
[40] *CRC Handbook of Chemistry and Physics*, edited by R. C. Weast and M. J. Astle, 62nd ed. (CRC, Boca Raton, 1981).
[41] P. Villars, *Pearson's Handbook of Crystallographic Data for Intermetallic Phases* (ASM International, Materials Park, Ohio, 1995).
[42] D. E. Partin, D. J. Williams, and M. O'Keeffe, J. Solid State Chem. **132**, 56 (1997).
[43] *Landolt-Börnstein Tables*, Landolt-Börnstein, New Series, Group III Vol. 7, Pt. b1, edited by K.-H. Hellwege and A. M. Hellwege (Springer, Berlin, 1975).
[44] *CRC Handbook of Chemistry and Physics*, edited by D. R. Lide, 73rd ed. (CRC, Boca Raton, 1992–1993).
[45] P. Hohenberg and W. Kohn, Phys. Rev. **136**, B864 (1964).
[46] B. Delley, J. Chem. Phys. **113**, 7756 (2000); **92**, 508 (1990), for N_2 and O_2, the wave functions are expanded in terms of a double-numerical quality localized basis set with a cutoff radius of 20 Bohr.
[47] C. Kittel, *Introduction to Solid State Physics* (Wiley, New York, 1986).
[48] R. W. G. Wyckoff, *Crystal Structures* (Wiley, New York, 1963), Vol. I.
[49] *CRC Handbook of Chemistry and Physics*, edited by R. C. Weast, M. J. Astle, and W. H. Beyer, 68th ed. (CRC, Boca Raton, 1987).
[50] J. P. Perdew, K. Burke, and M. Ernzerhof, Phys. Rev. Lett. **77**, 3865 (1996).
[51] *CRC Handbook of Chemistry and Physics*, edited by D. R. Lide, 77th ed. (CRC, Boca Raton, 1997).
[52] K. P. Huber and G. Herzberg, *Molecular Spectra and Molecular Structure IV: Constants of Diatomic Molecules* (Van Nostrand Reinhold, New York, 1979).
[53] C. H. Park and D. J. Chadi, Phys. Rev. B **55**, 12995 (1997).
[54] J. Neugebauer and C. G. Van de Walle, Appl. Phys. Lett. **68**, 1829 (1996).
[55] J. Neugebauer and C. G. Van de Walle, *Gallium Nitride and Related Materials*, MRS Symposia Proceedings No. 395 (Materials Research Society, Pittsburgh, 1996), p. 645.
[56] J. Neugebauer and C. G. Van de Walle, J. Appl. Phys. **85**, 3003 (1999).
[57] A. Fara, F. Bernardini, and V. Fiorentini, J. Appl. Phys. **85**, 2001 (1999).
[58] J. A. Chisholm and P. D. Bristowe, J. Phys.: Condens. Matter **13**, 8875 (2001).
[59] C. G. Van de Walle, Phys. Rev. B **57**, R2033 (1998).
[60] P. Boguslawski and J. Bernholc, Phys. Rev. B **56**, 9496 (1997).
[61] X. M. Duan and C. Stampfl, Phys. Rev. B **77**, 115207 (2008).
[62] H. Katayama-Yoshida, T. Nishimatsu, T. Yamamoto, and N. Orita, J. Phys.: Condens. Matter **13**, 8901 (2001), and references therein.
[63] R. Y. Korotkov, J. M. Gregie, and B. W. Wessels, Appl. Phys. Lett. **78**, 222 (2001).
[64] G. Kipshidze, V. Kuryatkov, B. Borisov, Y. Kudryavtsev, R. Asomoza, S. Nikishin, and H. Temkin, Appl. Phys. Lett. **80**, 2910 (2002).
[65] T. Yamamoto and H. Katayama-Yoshida, Jpn. J. Appl. Phys., Part 2 **36**, L180 (1997).
[66] S. H. Wei and S. B. Zhang, Phys. Rev. B **66**, 155211 (2002).
[67] L. G. Wang and A. Zunger, Phys. Rev. Lett. **90**, 256401 (2003).
[68] Y. Yan, J. Li, S. H. Wei, and M. M. Al-Jassim, Phys. Rev. Lett. **98**, 135506 (2007).
[69] R. Kalish, C. Saguy, C. Cytermann, J. Chevallier, Z. Teukam, F. Jomard, T. Kociniewski, D. Ballutaud, J. E. Butler, C. Baron, and A. Deneuville, J. Appl. Phys. **96**, 7060 (2004).
[70] M. Joseph, H. Tabata, and T. Kawai, Jpn. J. Appl. Phys., Part 2 **38**, L1205 (1999).
[71] D. C. Look, B. Claflin, Y. I. Alivov, and S. J. Park, Phys. Status Solidi A **201**, 2203 (2004).
[72] A. F. Wright, J. Appl. Phys. **96**, 2015 (2004).
[73] A. Uedono, S. F. Chichibu, M. Higashiwaki, T. Matsui, T. Ohdaira, and R. Suzuki, J. Appl. Phys. **97**, 043514 (2005).
[74] B. A. Hull, S. E. Mohney, H. S. Venugopalan, and J. C. Ramer, Appl. Phys. Lett. **76**, 2271 (2000).
[75] The calculations of the binding energies, with respect to the Mg acceptor and the O donor, of the defect complexes MgO_n ($n=1-4$) and Mg_mO ($m=2-4$) show that including In 4*d* electrons as valence electrons vs the nlcc treatment yield consistent results. Specifically, the binding energies (in eV) obtained including the In 4*d* electrons as valence and with the nlcc treatment (in brackets) are for MgO: 0.26 (0.42); MgO_2^+ 0.49 (0.68); MgO_3^{2+} 0.68 (0.77); and MgO_4^{3+} 0.75 (0.70). Importantly, the clustering of Mg and O is still favored with the inclusion of In 4*d* electrons. The atomic relaxations also exhibit similar trends: e.g., for O_N, In 4*d* and nlcc give 3.1% and 1.8% change in the average In-O bond length, respectively; for Mg_{In}, In 4*d* and nlcc yield −2.5% and −3.3% change in the average distance between Mg and N atoms; for the Mg_4O complex, In 4*d* and nlcc yield a Mg-O bond length of 2.06 and 2.04 Å, respectively; for the MgO_4 complex, In 4*d* and nlcc yield the same Mg-O bond length of 2.04 Å.
[76] C. H. Seager, A. F. Wright, J. Yu, and W. Götz, J. Appl. Phys. **92**, 6553 (2002).
[77] C. H. Seager, D. R. Tallant, J. Yu, and W. Götz, J. Lumin. **106**, 115 (2004).
[78] A. Armstrong, A. R. Arehart, D. Green, U. K. Mishra, J. S. Speck, and S. A. Ringel, J. Appl. Phys. **98**, 053704 (2005).
[79] For codoping of InN with Si and C, we verified that the two most stable complexes SiC and Si_2C behave consistently when both including In 4*d* electrons as valence and nlcc approach. Specifically, the binding energies (in eV) obtained including the In 4*d* electrons as valence and with the nlcc treatment (in brackets) are for SiC 0.41 (0.61), Si_2C 0.32 (0.40), and $(Si_2C)^+$ 0.23 (0.42). The atomic relaxations also exhibit similar trends: e.g., for Si_{In}, In 4*d* and nlcc yield −16% and −15.6% change in the average Si-N bond length, respectively; for C_N, both In 4*d* and nlcc yield a change in the In-O distance within 1%.
[80] C. Stampfl and C. G. Van de Walle, Phys. Rev. B **59**, 5521 (1999).
[81] M. Usuda, N. Hamada, K. Shiraishi, and A. Oshiyama, Jpn. J. Appl. Phys., Part 2 **43**, L407 (2004).